The Journal of Immunology

Rituximab-CD20 Complexes Are Shaved from Z138 Mantle Cell Lymphoma Cells in Intravenous and Subcutaneous SCID Mouse Models

Yongli Li, Michael E. Williams, John B. Cousar, Andrew W. Pawluczkowycz, Margaret A. Lindorfer and Ronald P. Taylor

J Immunol 2007; 179:4263-4271; ;
doi: 10.4049/jimmunol.179.6.4263
http://www.jimmunol.org/content/179/6/4263

The Journal of Immunology is published twice each month by
The American Association of Immunologists, Inc.,
1451 Rockville Pike, Suite 650, Rockville, MD 20852

Print ISSN: 0022-1767 Online ISSN: 1550-6606.

Rituximab-CD20 Complexes Are Shaved from Z138 Mantle Cell Lymphoma Cells in Intravenous and Subcutaneous SCID Mouse Models[1]

Yongli Li,* Michael E. Williams,† John B. Cousar,‡ Andrew W. Pawluczkowycz,* Margaret A. Lindorfer,* and Ronald P. Taylor[2]*

Infusion of standard-dose rituximab (RTX) in chronic lymphocytic leukemia (CLL) patients promotes rapid complement activation and deposition of C3 fragments on CLL B cells. However, immediately after RTX infusions, there is substantial loss (shaving) of CD20 from circulating malignant cells. Because shaving can compromise efficacies of anticancer immunotherapeutic mAbs, we investigated whether shaving occurs in SCID mouse models. Z138 cells, a B cell line derived from human mantle cell lymphoma, were infused i.v. or s.c. The i.v. model recapitulates findings we previously reported for therapeutic RTX in CLL: i.v. infused RTX rapidly binds to Z138 cells in lungs, and binding is accompanied by deposition of C3 fragments. However, within 1 h targeted cells lose bound RTX and CD20, and these shaved cells are still demonstrable 40 h after RTX infusion. Z138 cells grow in tumors at s.c. injection sites, and infusion of large amounts of RTX (0.50 mg on each of 4 days) leads to considerable loss of CD20 from these cells. Human i.v. Ig blocked shaving, suggesting that FcγRI on cells of the mononuclear phagocytic system promote shaving. Examination of frozen tumor sections from treated mice by immunofluorescence revealed large areas of B cells devoid of CD20, with CD20 intact in adjacent areas; it is likely that RTX had opsonized Z138 cells closest to capillaries, and these cells were shaved by monocyte/macrophages. The shaving reaction occurs in neoplastic B cells in tissue and in peripheral blood, and strategies to enhance therapeutic targeting and block shaving are under development. ***The Journal of Immunology,*** **2007, 179: 4263–4271.**

The use of mAbs in the rational targeting of epitopes on malignant cells has led to notable advances in treatment of certain forms of cancer (1–8); however, these therapies rarely lead to definitive cures. Multiple independent mechanisms may be operative which explain why greater levels of therapeutic efficacy are not achieved with mAb-based therapies. A detailed understanding of mAb-mediated tumor cell killing is required; specifically, does the mAb kill the cells directly, or does mAb-mediated killing require effector functions such as Ab-dependent cellular cytotoxicity (ADCC),[3] phagocytosis by monocytes or macrophages, and complement-dependent cytotoxicity (CDC) (3, 7, 8).

A voluminous literature, based on in vitro experiments, studies in mouse models, and clinical investigations, has revealed that anti-CD20 mAbs such as rituximab (RTX) kill targeted B cells by a combination of ADCC, phagocytic uptake, and/or CDC (9–22). It is important to recognize that these mechanisms can be saturated or exhausted under conditions of high tumor burden. If these mechanisms are exhausted, then infusion of large amounts of RTX in a patient with chronic lymphocytic leukemia (CLL) may not achieve therapeutic efficacy (2, 23), even though such infusions will lead to high steady-state concentrations of RTX in the bloodstream (24). In fact, our clinical investigations of the effects of RTX infusion in CLL have demonstrated that standard-dose RTX (375 mg/m^2) can substantially deplete complement for extended periods (25). Moreover, after infusion of standard-dose RTX, or even after infusion of moderate amounts (~100 mg) of the mAb, large numbers of targeted B cells are cleared from the bloodstream, most likely by liver macrophages. However, the ability of the infused RTX to promote clearance of additional B cells that re-equilibrate from bone marrow and lymphatics appears to be considerably diminished, most likely due to saturation of effector clearance mechanisms (21, 25). As a consequence, circulating RTX-opsonized cells are redirected to a second pathway in which RTX and CD20 are shaved off circulating cells; based on our in vitro model, the reaction appears to be promoted by effector cells that express FcγR (26).

The shaving reaction could substantially compromise the therapeutic efficacy of RTX; therefore, we established a mouse model to investigate shaving, with a goal of evaluating strategies focused on suppressing or at least minimizing the effects of this reaction. In this article, we show that Z138 cells, CD20$^+$ B cells derived from a human mantle cell lymphoma (27–29), rapidly grow and are tumorigenic when injected i.v. or s.c. in SCID mice. We have also previously reported, in an in vitro model, that RTX-opsonized Z138 cells, as well as other RTX-opsonized CD20-expressing cells

*Department of Biochemistry and Molecular Genetics, †Division of Hematology/Oncology and Hematologic Malignancy Program and Department of Medicine and Cancer Center, and ‡Department of Pathology, University of Virginia School of Medicine, Charlottesville, VA 22908

Received for publication February 9, 2007. Accepted for publication July 1, 2007.

The costs of publication of this article were defrayed in part by the payment of page charges. This article must therefore be hereby marked *advertisement* in accordance with 18 U.S.C. Section 1734 solely to indicate this fact.

[1] This study was supported by the Lymphoma Research Foundation Mantle Cell Lymphoma Grant (to M.E.W.) and the University of Virginia Cancer Support Grant.

[2] Address correspondence and reprint requests to Dr. Ronald P. Taylor, Department of Biochemistry and Molecular Genetics, University of Virginia Health Sciences Center, P.O. Box 800733, Charlottesville, VA 22908-0733. E-mail address: rpt@virginia.edu

[3] Abbreviations used in this paper: ADCC, antibody-dependent cellular cytotoxicity; Al, Alexa; bt, biotinylated; CLL, chronic lymphocytic leukemia; MESF, molecules of equivalent soluble fluorochrome; PI, propidium iodide; RTX, rituximab; CDC, complement-dependent cytotoxicity; IVIG, intravenous Ig.

including Raji and ARH77, are all subject to shaving by model monocyte/macrophages such as THP-1 cells (26). In this reaction, both RTX and CD20 are taken up and internalized by these acceptor cells.

We find that when RTX is injected into SCID mice after tumors with Z138 cells are established, substantial shaving of CD20 from these cells occurs in both i.v. and s.c. tumor models. The pattern of shaving in the s.c. tumor model strongly suggests that cells in contiguous areas of tissue are shaved, likely reflecting accessibility of these areas to both RTX and to effector cells. Several of our findings have important implications in the evaluation of the efficacy of mAbs in cancer immunotherapy and provide insight into mechanisms of response and resistance to these agents.

Materials and Methods

Antibodies

Mouse mAb 9H5, specific for human and mouse C3b/iC3b, was obtained by immunizing C3 knockout mice with human C3 (30). This mAb binds to Z138 cells opsonized with RTX and mouse serum and thus has a binding pattern similar to that of mAb 3E7 which binds to deposited C3b/iC3b on RTX-opsonized B cells in the presence of human serum (31). Rituximab (Biogen IDEC) was purchased at the hospital pharmacy. IgG1 mAbs HB43 and HB57, specific for the Fc region of human IgG and for the μ-chain of human IgM, respectively, have been reported (25, 32). $F(ab')_2$ of rat IgG2b mAb 2.4G2, specific for mouse FcγRII/III (33, 34) were prepared as described previously (30). HD1A, anti-human CD55, was a gift from Profs. P. Morgan and C. Harris (University of Wales, Cardiff, U.K.). Other reagents were obtained commercially: Mouse macrophage marker M1/70 (35) (American Type Culture Collection); polyclonal rabbit IgG anti-human CD20 (Lab Vision); Alexa (Al) Fluor 488 goat-anti-rabbit IgG, Al594 streptavidin (Molecular Probes); human PerCP CD45, human allophycocyanin CD19, biotinylated (bt) human CD59 (BD Biosciences); bt human CD45 (Caltag Laboratories); FITC mAb CL7503F, specific for all mouse C3 fragments, including C3dg (Cedarlane Laboratories). mAbs were labeled with biotin or Al dyes according to the manufacturers' instructions (Pierce and Molecular Probes).

In vivo protocol

Female 8- to 10-wk-old C.B-17/SCID mice were obtained from Harlan Breeders. All experiments were approved by the Institutional Animal Care and Use Committee. Studies were conducted in accordance with National Institutes of Health guidelines for animal care.

Z138 cells were cultured as described previously (28), washed in PBS, and 5×10^6 cells were administered either i.v. or s.c. Once tumor growth was evident (20–30 days), mice were either not treated or were given RTX i.v. (once) or i.p. (up to five injections on 5 consecutive days). In some experiments in the s.c. model, mice received separate i.p. injections of 300 μg of mAb 2.4G2 or its fragments, given each morning, and RTX 6 h later. Human intravenous Ig (IVIG; Baxter) was administered to mice (50 mg i.p (36)) in the morning of days 1 and 3 and RTX 6 h later on 4 consecutive days.

Analysis of tumor cells

Cell suspensions were prepared from lungs or solid tumors by digestion with a mixture of collagenase, hyaluronidase, elastase, and DNase (37, 38), purified by density gradient centrifugation (39), washed, and reconstituted in 2 mg/ml mouse IgG in BSA-PBS. Samples were stained as described below, and analyzed by flow cytometry, following procedures used previously to examine B cells from CLL patients (21, 25). Z138 cells were identified by gating on side scattering and PerCP CD45 alone or by gating with both PerCP CD45 and allophycocyanin CD19; both methods gave similar results. Z138 cells were assayed for total CD20 by incubation with excess RTX ex vivo, followed by either Al488- or PE-mAb HB43, which binds to the Fc region of RTX (25). Alternatively, no RTX was added ex vivo, and washed cells were stained with either mAb HB43 to measure bound RTX or with Al488 RTX to measure available CD20. The presumption in this last assay is that Al488 RTX will bind to nonligated CD20, but binding will not occur if CD20 is previously occupied by infused unlabeled RTX. Fluorescence analysis was performed with a FACSCalibur flow cytometer (BD Biosciences); fluorescence intensities were converted to molecules of equivalent soluble fluorochrome (MESF) (25). Several different Al-labeled mAb preparations were used in these experiments, giving rise to different MESF values for certain samples. In addition, we found that MESF values for ostensibly identical cell preparations varied moderately from day-to-day, and unless otherwise noted, all comparisons and evaluations are based on data sets accumulated for a single day's experiment.

Frozen sections (5 μm) of s.c. tumors were analyzed by fluorescence immunohistochemistry by staining with Al488 or Al594 mAbs, as previously described (39).

Preliminary calibrations

In each experiment, we measured CD20 levels on naive Z138 cells in parallel with CD20 levels on Z138 cells recovered from lungs or from s.c. tumors in SCID mice. In most cases, CD20 levels on recovered Z138 cells were reduced compared with levels on Z138 cells growing in culture. In 13 experiments conducted over a period of >12 mo, CD20 on Z138 cells recovered from lungs or s.c. tumors in untreated mice averaged 36 $\pm$ 23% (n = 11, mean $\pm$ SD, i.v. lung model, six separate experiments) and 31 $\pm$ 8% (n = 13, s.c. model, seven separate experiments) of CD20 levels on cells growing in culture. Based on a gating scheme in which Z138 cells growing in culture were set to 99% CD20 positive, a small fraction (~12%) of cells isolated from untreated mice was CD20 negative.

Statistics

Means were compared by t tests using Sigma Stat 3.1.

Results

The i.v. model: Z138 cells growing in lungs of RTX-treated SCID mice are shaved, and C3 fragments are deposited

Several SCID mouse-B cell lymphoma models are based on i.v. infusion of cells from a human B cell line (14, 40, 41), and we adapted these models to Z138 cells to evaluate effects of RTX infusion. Three to 4 wk after cells were injected i.v., mice showed evidence of tumor growth (modest lethargy or the start of hind leg paralysis) and they were either not treated, or were given RTX, and they were subsequently euthanized between 15 min and 3 days after RTX treatment. In the Daudi cell/SCID mouse models, Daudi cells grow in the lungs (40, 41), and we found that Z138 cells also grow in the lungs in the present model.

Z138 cells recovered from the lungs were identified based on positive CD45 and CD19 signals and side scattering (21). Z138 cells obtained from untreated mice take up substantial amounts of RTX when probed ex vivo, indicating that these cells express high levels of CD20. Representative histograms in Fig. 1*A* show comparable analyses for cells isolated from the lungs of mice that received i.v. RTX, followed by euthanization 15 or 60 min later. After 60 min, the level of CD20 on the Z138 cells is reduced considerably, compared with the level found in the untreated mouse. Moreover, as is evident in Fig. 1*A* (constant times for counting), fewer cells could be isolated from the RTX-treated mice, suggesting that there was a substantial level of RTX-induced killing, presumably mediated by complement (25).

The results in Fig. 1, *B–D*, demonstrate that soon (15 min) after i.v. infusion of RTX, substantial binding of this mAb to Z138 cells occurs, and binding is accompanied by complement activation, as manifested by deposition of mouse C3 fragments on the cells. However, findings in mice that were euthanized 1 h or more after RTX infusion reveal that most cell-bound RTX, as well as CD20, have been removed, and a substantial fraction of deposited C3 fragments is also removed. Based on MESF values for untreated vs treated mice, 84 $\pm$ 4% (mean $\pm$ SD) of CD20 on the Z138 cells was removed (shaved), 1–2 h after RTX infusion. Notably, even after 2 h, small amounts of RTX was still bound to cells; the signal obtained after probing with mAb HB43 alone is larger than that observed on Z138 cells taken from lungs of mice that received no RTX (2200 MESF units vs 200 MESF units). The trend of RTX binding, followed by C3 fragment deposition and then shaving of the CD20/RTX complex from the cell, was quite reproducible in

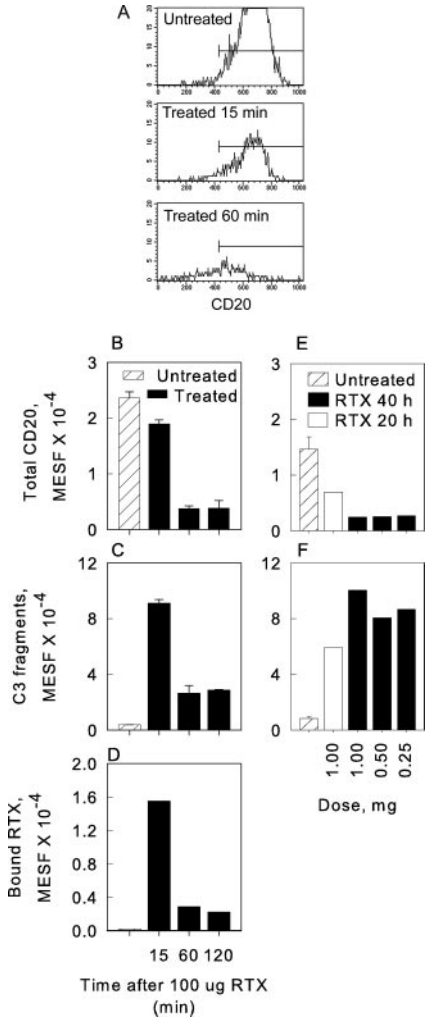

FIGURE 1. Effect of single i.v. RTX treatments on CD20 levels and C3 fragment deposition on Z138 cells recovered from the lungs of SCID mice 15 min to 40 h after RTX infusion. *A*, Human $CD19^+CD45^+$ Z138 cells were probed with RTX followed by PE mAb HB43. Representative histograms are presented for an untreated mouse and for mice that received 100 μg of RTX and were euthanized 15 or 60 min later. *B–F*, Quantitative flow cytometry results are presented as MESF. In the first, acute series, three mice received i.v. infusions of 100 μg of RTX and were, respectively, euthanized 15, 60 (see *A*), or 120 min later. *B*, Cells were probed to reveal total CD20, based on RTX followed by PE mAb HB43. Cells were analyzed in four replicates for each mouse, and the differences between the untreated control mouse and treated mice were significant at $p < 0.001$ for all three treated mice. *C*, Bound C3 fragments were assayed based on probing with a FITC rat mAb specific for all fragments of mouse C3. Three replicates were analyzed for each mouse, and differences between untreated and treated were significant at $p < 0.001$, $p = 0.002$, and $p < 0.001$ for the three treated mice. *D*, Bound RTX was measured based on direct probing with PE mAb HB43. *E* and *F*, In the longer term experiments, four mice were infused i.p. with between 0.25 and 1 mg of RTX, and they were then euthanized 20–40 h later. Three untreated controls were processed in parallel (striped bar). CD20 was measured based on probing with RTX, followed by Al488 mAb HB43. CD20 levels on Z138 cells of the three untreated mice averaged 20 ± 3% of CD20 levels on Z138 cells grown in culture. Differences between the average CD20 values in *E* and C3 fragment deposition in *F* for the three untreated mice compared with the three treated mice at 20 h were both significant at $p < 0.001$.

the mouse model, but the magnitude of effects showed some variability. For example, in another experiment, two mice each received 300 μg of RTX by i.v. infusion, and they were euthanized either 30 or 90 min later. CD20 levels on Z138 cells harvested from lungs of RTX-treated mice corresponded to 14,300 and 13,300 MESF units, respectively, compared with values of 37,200 for two untreated mice, thus giving 61 and 64% shaving, respectively. Some RTX was still bound to shaved cells; MESF signals after probing with Al488 mAb HB43 alone were 12,000 and 11,000 units, respectively, suggesting that one-third of the original CD20 on the Z138 cells was bound by RTX.

We next determined the effects of exposure of Z138 cells in the lungs to larger quantities of RTX over longer time periods. In these experiments, mice were euthanized 20–40 h after RTX infusion. Results in Fig. 1, *E* and *F*, demonstrate that recovered Z138 cells are again shaved, as evidenced by reduced levels of CD20 (shaving of 83 ± 2%). Moreover, fragments of mouse C3 are still found associated with these cells. This result, similar to our findings in CLL patients who received RTX (21), suggests that not all of the C3 fragments deposited on cells due to complement activation after RTX binding are removed when RTX-CD20 immune complexes are stripped off during the shaving reaction. Similar results with respect to shaving and C3 fragment deposition were obtained in experiments in which RTX was infused and mice were euthanized 70 h later (results not shown).

We and others (31, 42, 43) have reported that C3 activation fragments deposited on cancer cells can, in principle, be used as specific targets for cancer immunotherapy. mAb 3E7 recognizes cell-bound human C3b/iC3b and can bind to CD20-positive cells when they are opsonized with RTX either in vitro in normal human serum or in vivo in the circulation of nonhuman primates (31). To develop a mouse model for this paradigm, we immunized C3-deficient mice with human C3 and generated mAbs, including mAb 9H5, which recognize both human and mouse C3b/iC3b fragments. During opsonization of Z138 cells by RTX in the presence of mouse serum, mAb 9H5 can bind to deposited C3 fragments despite the presence of C3 fragments generated in the milieu (results not shown). Therefore, we tested the potential of mAb 9H5 to bind in vivo to Z138 cells after i.v. infusion of RTX. The results in Fig. 2 demonstrate that Al488 mAb 9H5, infused into the mice 16 h earlier, binds to lung-associated Z138 cells within 30 min after infusion of RTX, giving a signal of ~180,000 MESF units. In a parallel in vitro control, Z138 cells were opsonized with RTX or no mAb in the presence of 50% normal mouse serum and Al488 mAb 9H5 for 20 min at 37°C. In the presence of RTX, binding of Al488 mAb 9H5 corresponded to 370,000 MESF, and the signal was reduced to 30,000 MESF if RTX was omitted. Thus, the in vivo result for mAb 9H5 binding to RTX-opsonized cells in the presence of complement is within a factor of 2 of the result for the in vitro control.

In experiments in which only Al488 mAb 9H5 was infused (no treatment with RTX), binding of mAb 9H5 to Z138 cells was only slightly above background, indicating there are few C3 fragments present on Z138 cells isolated from mouse lungs if RTX is not infused. We also found that mAb 9H5 binds poorly in vitro to RTX-opsonized Z138 cells if it is reacted with cells taken from mice several hours after RTX infusion (data not shown). This finding suggests that most deposited C3b/iC3b is rapidly degraded to C3dg, but that if mAb 9H5 is present in the circulation before RTX infusion, it can bind to RTX-opsonized cells during complement activation, presumably soon after initial deposition of the C3b/iC3b.

Evaluation of absolute cell numbers: preliminary evaluation of RTX efficacy

Our experiments in the i.v. model were designed to determine whether single doses of RTX could bind to malignant B cells in the

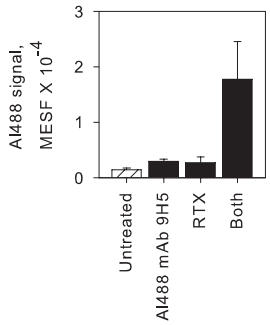

FIGURE 2. mAb 9H5, specific for mouse C3b, bound in vivo to Z138 cells in the lungs as a consequence of RTX treatment. Mice that had received Z138 cells i.v. were divided into four groups. The first group (n = 3) was not treated. The second group (n = 3) received 200 μg of Al488 mAb 9H5 i.p. and was euthanized 16 h later. The third group (n = 2) was injected i.v. with 250 μg of RTX and euthanized 30 min later. The last group (Both, n = 4) received 200 μg of Al488 mAb 9H5 i.p. and 15.5 h later was injected i.v. with 250 μg of RTX and euthanized 30 min later. For a given experiment, all groups were euthanized at the same time and the separate batches of cells were processed in parallel. $CD45^+CD19^+$ Z138 cells were identified and assayed for binding of infused Al488 mAb 9H5, based on the Al488 signal. Infusion of Al488 mAb 9H5 alone gave MESF values quite close to those of the untreated and RTX only mice, indicating that background C3 fragment deposition on the cells (in the absence of RTX) must be quite low. Differences between the mice that received both RTX and Al488 mAb 9H5 were significant compared with the other treatments at p = 0.015. Results of three experiments are averaged.

lungs, activate complement, and promote shaving, and thus did not focus on direct evaluation of RTX efficacy. However, in most cases we recovered far fewer Z138 cells from the lungs of RTX-treated mice compared with the number of cells recovered in untreated matched controls, thus indicating that although shaving occurred, some RTX efficacy was evident. Under conditions in which flow cytometry counting times were carefully controlled, in 21 of 23 cases the percentage of recovered cells for RTX-treated mice averaged 25 ± 14% (mean and SD; range, 10–64%) of the values obtained for untreated controls. In one case, equal numbers of cells were found for the matched mice, and in only 1 of 23 experiments did we recover more cells from a RTX-treated mouse than from a control.

The s.c. model: Z138 cells growing in solid tumors in SCID mice are shaved after RTX infusion

Z138 cells also grow in SCID mice when the cells are injected s.c.; this result confirms similar findings obtained in Rag2-M mice (28). Three to 4 wk after s.c. injections, frank tumors (~5 mm in diameter) were evident, and mice were either not treated, or received one or more i.p. doses of RTX, and were euthanized within 7 days. Z138 cells were recovered from s.c. tumors and analyzed by flow cytometry. Based on a threshold set to classify 99% of cultured Z138 cells as CD20 positive, and as noted in the preliminary calibrations, a fraction of the Z138 cells that grew in untreated SCID mice was classified as CD20 negative (Fig. 3*A*). In mice that received between one and three infusions of RTX, we observed a small but reproducible increase in the percentage of CD20 cells classified as CD20 negative. Based on MESF values for the entire population of cells, treatment with RTX led to modest shaving for the five pairs of matched mice illustrated in Fig. 3*A*; compared with untreated controls, RTX treatment led to shaving of 27 ± 8% of CD20.

The results in Fig. 3*A* could indicate that insufficient RTX was delivered to the tumors to induce substantial shaving. Therefore, in subsequent experiments, we increased the dose and frequency of RTX administration. Multiple infusions of RTX, at 500 μg/dose, promoted profound loss of CD20 from the Z138 cells. Representative dot plots and histograms, which compare Z138 cells in culture and Z138 cells recovered from an untreated and a RTX-treated mouse, indicate that the RTX treatments induced substantial loss of CD20, but did not affect CD19 (Fig. 3*B*). Results in Fig. 3*C*,

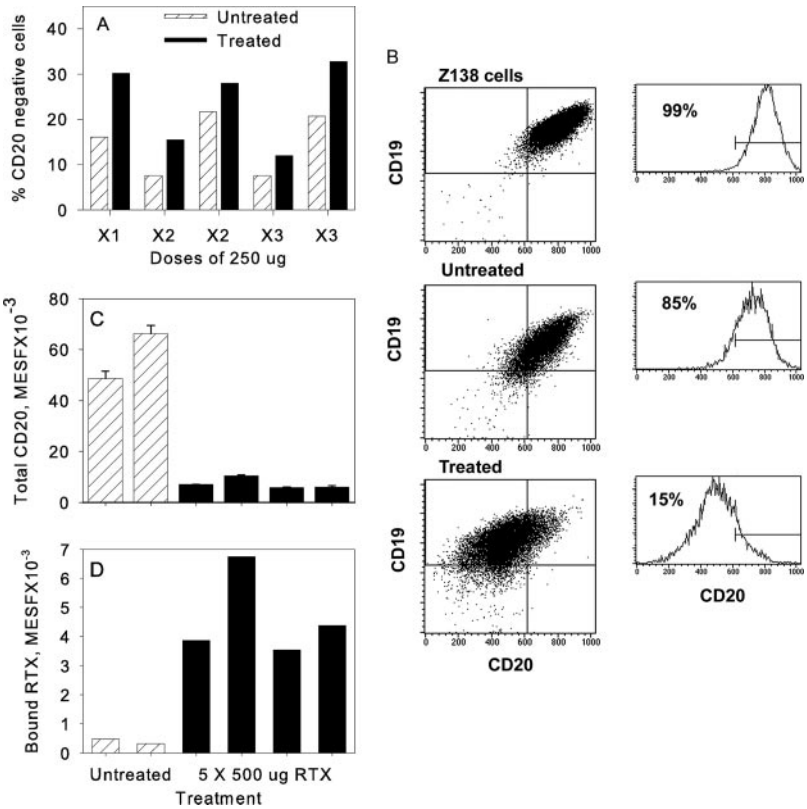

FIGURE 3. In the s.c. model, moderate doses of RTX increase the percentage of CD20-negative cells, but repeated higher doses induced substantial shaving. Tumor cells were harvested 1–2 days after final RTX infusions. *A*, Summation of data from five separate paired mice. In vitro-cultured Z138 cells were set as 1% negative for CD20 in each experiment, and the percentage of CD20-negative cells for matched untreated animals was compared with levels in mice that received RTX. In all cases, there were small increases in the percent negative as a consequence of RTX treatment. *B–D*, Four mice each received 500 μg of RTX on 5 consecutive days and were euthanized 2 days after the last RTX infusion. $CD45^+$ Z138 cells were also identified based on side scatter and were examined for CD19 and for CD20. Representative dot plots and histograms are displayed for Z138 cells (grown in culture), compared with Z138 cells isolated from an untreated mouse, or isolated from a RTX-treated mouse. In all cases, CD20 was determined by probing with RTX followed by PE mAb HB43. CD19 levels are preserved after RTX treatment, but CD20 is substantially reduced, leaving only 15% of the cells expressing significant levels of CD20. *C* and *D*, Total CD20 (*C*, four separate determinations for each mouse) and bound RTX (*D*, single determinations) were, respectively, measured by probing with PE mAb HB43 with and without ex vivo treatment with excess RTX, and thus *D* allows for an estimate of the relative amount of bound RTX after treatment. *C* and *D*, Differences between the averages for the untreated compared with treated mice were significant at $p < 0.001$ and p = 0.019, respectively.

based on MESF units, reveal that >85% of CD20 was removed from cells as a consequence of multiple treatments with RTX. To determine whether residual RTX was bound to the cells, they were also probed with mAb HB43 alone, without any ex vivo opsonization with excess RTX. A small amount of background binding of mAb HB43 was detected on Z138 cells taken from mice not treated with RTX (two striped bars, Fig. 3*D*). However, in RTX-treated mice, a modest but statistically significant ($p = 0.019$) higher level binding of mAb HB43 was demonstrable (Fig. 3*D*, four solid bars). Finally, comparison of the MESF values for mAb HB43 binding obtained for ex vivo RTX-opsonized cells in untreated mice (Fig. 3*C*, an average of 57,000 MESF units for total CD20) to the corresponding values for RTX-treated mice in Fig. 3*D* (MESF values of 3,500–6,700 for bound RTX) indicate that in mice infused with RTX, 5–10% of total CD20 sites (before RTX infusion) on the Z138 cells contained bound RTX.

Effects of anti-FcγRII/III mAb 2.4G2 on shaving in the s.c. model

Our in vitro model of the shaving reaction demonstrated that Fcγ receptors play a key role in the process (26). Therefore, we attempted to block Fcγ receptors in the mouse model by treating mice with mAb 2.4G2, which is specific for FcγRII/FcγRIII (33, 34). The results in Fig. 4*A* indicate that five infusions of 250 μg of RTX induced 80% loss of CD20 on Z138 cells recovered from SCID mice. Moreover, treatment of mice with multiple infusions of either intact or $F(ab')_2$ of mAb 2.4G2 had modest effects in blocking RTX-mediated shaving. We directly probed washed cells with Al488 RTX to provide an independent test for availability of CD20 on Z138 cells. The results indicate that in untreated mice, CD20 is indeed available for binding by Al488 RTX (MESF signal of 80,000–100,000). However, much less Al488 RTX binds to Z138 cells in RTX-treated mice (MESF values of 20,000 for RTX or RTX plus mAb 2.4G2 $F(ab')_2$, corresponding to ~80% shaving). Since comparable amounts of shaving were observed based on either an indirect assay (excess RTX followed by Al488 mAb HB43, total CD20) or based on direct probing with Al488 RTX, it is very unlikely that CD20 epitopes are simply masked by infused RTX. After ex vivo reaction with Al488 RTX, we obtained MESF values of 27,000 for mice that received RTX plus intact mAb 2.4G2, indicating that the intact mAb modestly blocked shaving, in agreement with results in Fig. 4*A*, which are based on determination of total CD20. Finally, for all mice used in the experiments illustrated in Fig. 4*A*, aliquots of cells were stained with PerCP CD45, allophycocyanin CD19, and propidium iodide (PI) to determine whether isolated Z138 cells were alive. In all cases, we detected a low level of staining of Z138 cells with PI, indicating that >85% of recovered Z138 cells were alive, for both RTX-treated and nontreated mice.

IVIG blocks shaving in the s.c. model

We next attempted to block the shaving reaction by infusing large amounts of human IVIG (36, 44) into mice before initiating RTX treatments. Mice then received RTX and were compared with mice that received RTX and were pretreated with either intact or $F(ab')_2$ of mAb 2.4G2. The results in Fig. 4, *B* and *C*, in agreement with Fig. 4*A*, again demonstrate that neither mAb 2.4G2 nor its fragments can effectively block RTX-mediated shaving. However, two treatments with IVIG largely inhibited RTX-induced loss of CD20. To determine whether human IVIG infused in mice might have interfered with binding of mAb HB43 to RTX-opsonized cells, we probed cells directly with Al488 RTX. This mAb bound at high levels to Z138 cells of mice that received both RTX and IVIG, and binding was comparable to that observed in untreated mice (Fig. 4*C*), providing additional evidence that IVIG blocks shaving that would otherwise be induced by RTX. Finally, in all experiments described in Figs. 3 and 4, we found no evidence for deposition of mouse C3 fragments on Z138 cells in either untreated or RTX-treated mice, thus indicating there was little complement activation when RTX targeted Z138 cells in the s.c. compartment.

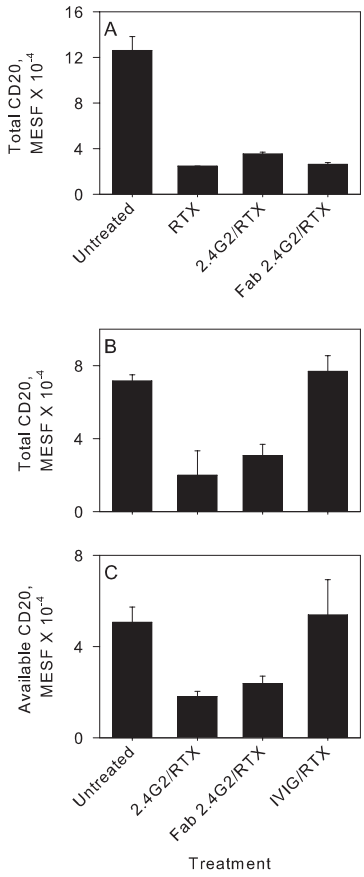

FIGURE 4. In the s.c. model, RTX-mediated shaving of CD20 is weakly blocked by anti-FcγRII/III mAb 2.4G2 but not by its $F(ab')_2$, and shaving is inhibited by human IVIG. *A*, Mice were either untreated ($n = 3$) or received 250 μg of RTX on 5 consecutive days ($n = 2$) or they received the same amount of RTX as well as six infusions, 300 μg each, of mAb 2.4G2 ($n = 2$) or its $F(ab')_2$ ($n = 2$); the infusions of mAb 2.4G2 were started 1 day earlier than RTX treatment. Starting the second day, mAb 2.4G2 was first infused, and RTX was infused 6 h later. *B* and *C*, Mice were either untreated ($n = 2$), or received 250 μg of RTX on 4 consecutive days as well as four infusions of either 300 μg of mAb 2.4G2 or its $F(ab')_2$ (two mice in each case), or on days 1 and 3, 50 mg of IVIG ($n = 3$). Total CD20 (*A* and *B*) was measured as in Fig. 3. *C*, The cells were probed directly with Al488 RTX to measure available CD20. Representative of results of two similar experiments, each with nine mice. *A*, Differences between untreated and the three respective groups of RTX-treated mice (*left* to *right*) were $p < 0.001$, $p = 0.014$, and $p = 0.002$. Treatment with mAb 2.4G2 and RTX led to a small but statistically significant difference compared with RTX alone, $p = 0.014$. *B*, Differences between untreated and treatment with either 2.4G2 plus RTX or 2.4G2 fragments plus RTX were significant, $p = 0.034$ and $p = 0.014$, respectively. *C*, The same comparisons also gave significant differences, $p = 0.022$ and $p = 0.035$.

Immunohistochemical evidence for shaving of contiguous regions of cells

The results in the s.c. model reveal an interesting dose-response and time-dependent reaction for RTX-induced loss of CD20. Noteworthy is demonstration of increases in CD20-negative cells induced by infusions of relatively small amounts of RTX (Fig. 3*A*).

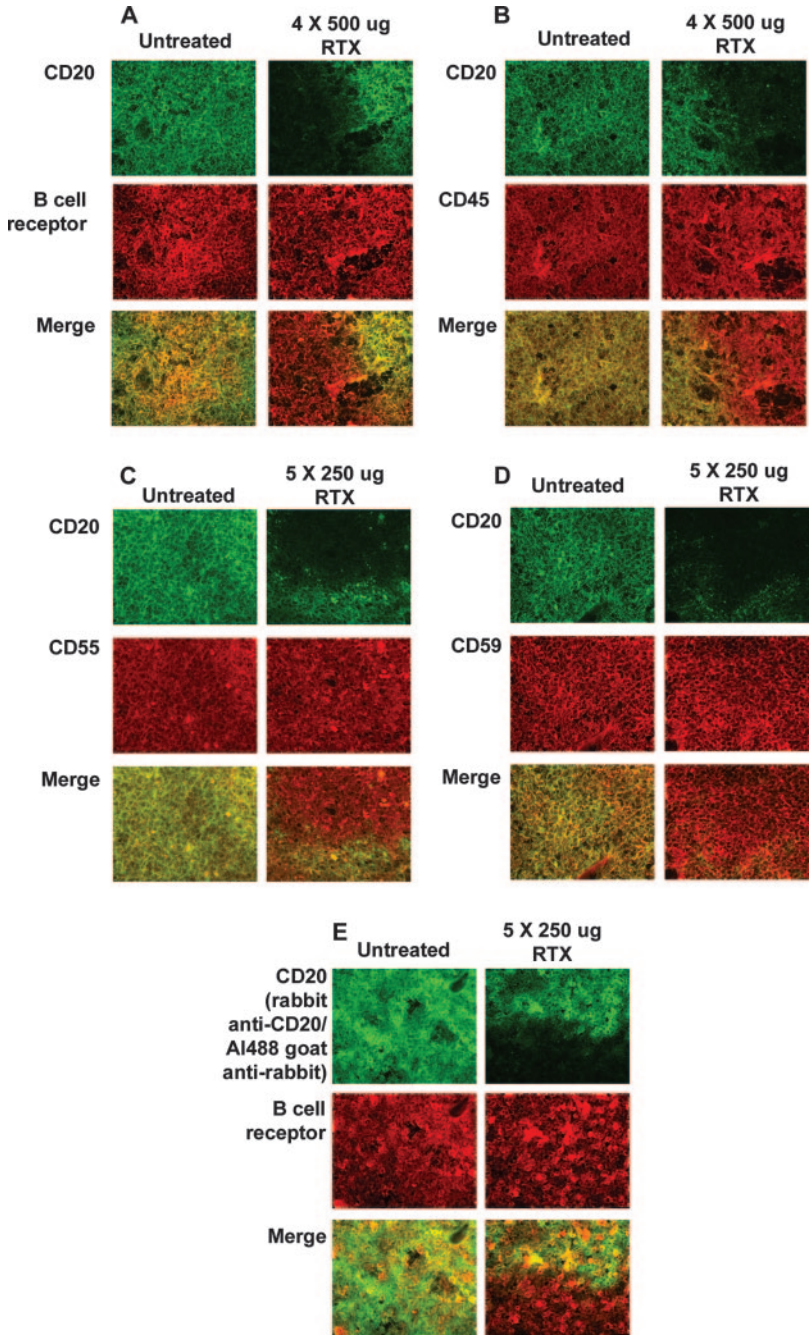

FIGURE 5. RTX-mediated shaving of CD20 of cells in discrete and contiguous areas is demonstrable in s.c. tumors based on fluorescence immunohistochemistry analyses of frozen sections. Subcutaneous tumors were harvested from untreated mice (*left side* of each panel) or from a mouse treated 4 consecutive days with 500 μg of RTX (*right side*, *A* and *B*) or from a mouse treated 5 consecutive days with 250 μg of RTX (*right side*, *C–E*). *A*, Sections were stained for total CD20 (RTX followed by Al488 mAb HB43, green signal) and for the human BCR (Al594 mAb HB57, red signal), and the individual and merged images are displayed. *B–D*, Total CD20 was evaluated in a similar fashion, and CD45, CD55, and CD59 (red signals) were revealed by consecutive staining with specific bt mAbs followed by streptavidin-Al594. Use of isotype controls for the CD-specific bt mAbs produced no red signal (data not shown). *E*, Sections were stained for total CD20 based on consecutive probing with rabbit IgG anti-human CD20 followed by Al488 goat anti-rabbit IgG, and the BCR was revealed as in *A*. Olympus BX40 fluorescent microscope and Olympus Magnafire Digital Camera; original magnification, ×40.

It is possible that after lower RTX doses only cells closest to capillaries bind RTX and interact with effector cells that can promote shaving. On this basis, it is likely that as the doses and frequency of RTX infusions are increased, more cells targeted by RTX are shaved, but there still could be other untouched regions (presumably furthest from capillaries) in which CD20 on Z138 cells is substantially preserved. To test this possibility, we examined frozen sections of s.c. tumors by fluorescence immunohistochemistry. Tissue was stained for CD20 with excess RTX, followed by Al488-labeled mAb HB43, and with one of a number of other B cell markers. The results, illustrated in Fig. 5, *A–D*, and representative of experiments on four different RTX-treated mice and five untreated controls, have a common theme: both CD20 and other B cell markers are easily demonstrable when cells from untreated mice are examined. However, B cells analyzed in sections taken from s.c. tumors in mice treated with multiple doses of RTX have defined areas which express little, if any, CD20, while still expressing normal levels of the human BCR, CD45, CD55, and CD59. Loss of CD20 in tissue sections of RTX-treated mice is in fact demonstrable by an alternative probing scheme (Fig. 5*E*). Frozen sections from RTX-treated mice and untreated controls were stained with a polyclonal rabbit IgG Ab preparation specific for CD20, followed by Al488 goat anti-rabbit IgG; in treated animals, the Z138 cells again showed loss of CD20, but preservation of the BCR.

We also used single-color immunohistochemistry to test frozen sections for shaving. The results, illustrated in Fig. 6, are based on probing samples with either primary bt probes or with unlabeled primary probes followed by secondary bt developing agents. We again found that compared with frozen sections isolated from untreated mice, comparable sections from RTX-treated mice expressed the same patterns: large areas were almost totally devoid of CD20, but

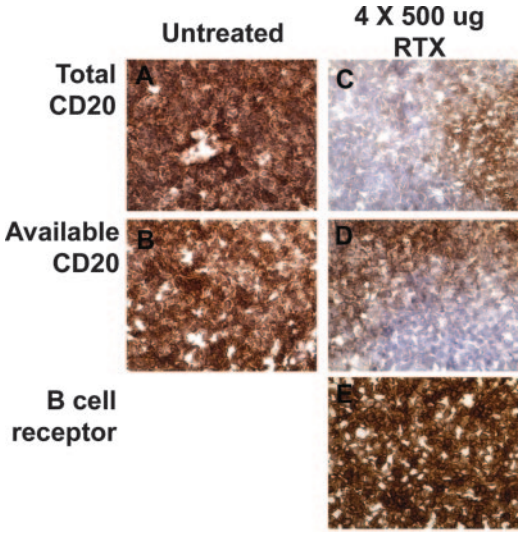

FIGURE 6. Single-color immunohistochemistry analyses of frozen sections from the s.c. model also revealed shaving of CD20. Sections of tumor from an untreated mouse (*left side*) were compared with sections from a mouse that received four infusions of 500 μg of RTX. Total CD20 (*A* and *C*) was revealed by consecutive probing with RTX followed by bt mAb HB43, and then the slides were developed with Vectastain Elite ABC reagent (Vector Laboratories), with 3,3′-diaminobenzidine substrate followed by hematoxylin. Available CD20 (*B* and *D*) and the BCR (*E*) were, respectively, revealed by probing with btRTX and btmAb HB57, followed by the same development protocol.

the BCR was ubiquitously expressed throughout cells in the sections. The same pattern of shaving was observed by assaying directly for binding of btRTX or indirectly by adding excess unlabeled RTX followed by btHB43. Therefore, as noted previously, based on tests for binding of Al488 RTX (Fig. 5), the low level of binding of exogenously added btRTX to Z138 cells taken from s.c. tumors of RTX-treated mice was not due to masking of the CD20 epitope by bound RTX, but rather indicates that CD20 was indeed shaved.

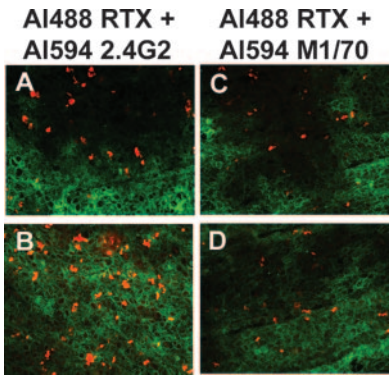

FIGURE 7. In the s.c. model, mouse macrophages are demonstrated in both shaved and nonshaved sections of frozen tissue after RTX treatment (5 × 250 μg of RTX) as revealed by fluorescence immunohistochemistry. *A* and *B*, Cells were stained with Al488 RTX and with Al594 mAb 2.4G2, specific for mouse macrophage FcγRII/III. *C* and *D*, Cells were stained with Al488 RTX and with Al594 mAb M1/70, specific for CR3 on mouse macrophages. The stained sections are not consecutive and were selected to represent either shaved or nonshaved regions of cells. The signal due to M1/70 (*right side*) is weaker, but macrophages are demonstrable in these sections. In each case, the merged images RTX and 2.4G (*A* and *B*) or RTX and M1/70 (*C* and *D*) are shown. Original magnification, ×40. Mouse macrophages can be seen in both the shaved (*A* and *C*) and CD20-rich (*B* and *D*) regions.

Our previous in vitro experiments suggest that monocyte/macrophages play a key role in the shaving reaction (26). Fluorescence immunohistochemistry analyses were performed on frozen sections of s.c. tumors based on the use of two different macrophage markers, 2.4G2 and M1/70. These markers reveal that macrophages are present in fields of both shaved and unshaved Z138 cells (Fig. 7) in tissue taken from a RTX-treated mouse. Finally, microscopic examination of formalin-fixed sections confirmed our findings based on PI staining: most (>85%) Z138 cells were alive in both naive and RTX-treated animals. Macrophages were clearly present in areas of tumor that had predominantly Z138 cells in tissue sections taken from both untreated and RTX-treated mice (data not shown).

Discussion

The present studies, which investigate the action of RTX on CD20-positive Z138 human mantle cell lymphoma cells in i.v. and s.c. mouse models, replicate several of our key findings on the fate of circulating B cells in CLL patients after RTX infusion (21, 25). In the i.v. model (Figs. 1 and 2), binding of RTX promoted rapid activation of complement and deposition of C3 activation fragments; soon after RTX binds to the cells, a large fraction of this mAb, CD20 and deposited C3 activation fragments, is removed from B cells in a process we have called the shaving reaction. However, some C3 fragments are preserved on cells even after levels of CD20 are substantially reduced. We have reported that in CLL patients these C3 fragments persist on circulating shaved (very low CD20) B cells for periods of at least 48 h (21), and a similar pattern is evident in the mouse model upon analysis of Z138 cells taken from lungs 20–40 h after RTX infusion. Also in common with our observations in CLL, C3 fragments deposited on the Z138 cells have been degraded to C3dg, because Al488 mAb 9H5, specific for C3b/iC3b, only bound to Z138 cells if it was infused before RTX treatment (Fig. 2).

The s.c. model had several similarities, but also notable differences when compared with the i.v. model. In the s.c. model, we did not perform any acute experiments, because we presumed that a longer period of time would be required for i.p. RTX to enter the tumor and interact with Z138 cells. Indeed, 24 h after RTX infusion, the mAb had partially penetrated the tumors; after relatively small amounts of RTX were administered, flow cytometry analyses suggested that a fraction of Z138 cells had lost CD20 due to RTX-promoted shaving (Fig. 3*A*). Larger and repeated doses of RTX led to a high degree of shaving, although small amounts of residual cell-bound RTX were clearly evident on the cells (Fig. 3, *C* and *D*). However, in the s.c. model, cells targeted by RTX showed no evidence for deposition of C3 fragments, and although Z138 cells were accessible to RTX, the results suggest that one or more complement proteins were excluded from the tumor. This finding has potential implications with respect to use of mAbs for targeting of lymphomas and solid tumors in humans. If in vitro experiments were to indicate that complement-dependent cytotoxicity afforded one of the mechanisms of tumor killing mediated by the mAb, then it would be important to determine whether complement activation could occur in the tumor microenvironment.

Our present results in the s.c. model, taken along with in vitro findings (26), demonstrate that cells can be shaved after binding of the IgG mAb RTX and that complement is not required to promote shaving. However, in both cases, large amounts of IgG can inhibit shaving. Our in vitro studies suggest that complement activation and C3b deposition can suppress the inhibitory action of IgG, possibly by modulating interaction between the opsonized cells and FcγRI. Alternatively, the C3 fragments deposited on the RTX-opsonized substrate cells may provide ligands such as iC3b which can engage CR3 on effector cells (35), thus enhancing cell-cell

contact and promoting shaving, even in the presence of IgG. In future studies we hope to determine whether IVIG can block shaving in the i.v. model; in this system complement activation can occur and thus potentially overcome the inhibitory effect of IVIG.

Our previous in vitro investigations provided strong evidence that the shaving reaction requires recognition of cell-bound RTX by FcγR on effector cells, and the evidence most strongly implicated the high-affinity receptor FcγRI (26). Our observation that large amounts of IVIG, but not mAb 2.4G2 (specific for FcγRII/III) could block shaving in the mouse model (Fig. 5) provides additional evidence suggesting that the high-affinity receptor on mouse macrophages mediates shaving in the present model, although we cannot definitively exclude a role for the recently described FcγRIV (45).

The standard dose of RTX that is used in CLL at first efficiently targets and clears circulating B cells. This process occurs as a result of opsonization, thus potentially allowing both killing mediated by FcγRIII on NK cells (46–50) and clearance mediated by FcγR on liver and possibly splenic macrophages (15, 17, 22, 51–53). However, our clinical investigations suggest that as more B cells enter the circulation after this first pass clearance, these B cells are also opsonized with RTX, but they are not cleared, presumably because of saturation of the mononuclear phagocytic system by previously cleared cells (21, 25). This saturation phenomenon may in part reflect down-regulation/internalization of FcγRIII due to processing of large numbers of RTX-opsonized cells (49, 53). Then, the "second wave" of RTX-opsonized cells appears to be diverted to a different pathway, resulting in shaving. It is therefore possible that large amounts of either IVIG, or simply an irrelevant isotype control human IgG1 mAb, could be used to block FcγRI and thus inhibit shaving in CLL patients treated with RTX.

Our analyses of shaving, based on examination of frozen tissue sections of tumors by fluorescence and classical immunohistochemistry (Figs. 5–7), may have important implications with respect to identifying factors that limit the effectiveness of mAbs in targeting solid tumors. The results demonstrate that RTX induces shaving and reinforce our flow cytometry findings. Figs. 5–6 provide compelling evidence that RTX treatment leads to generation of large and contiguous areas of tumor cells that have lost CD20. These findings can be reasonably interpreted in terms of the accessibility of tumor cells to infused mAbs, such as RTX (54, 55). Cells closest to capillaries would be expected to be those first bound by RTX and then the mAb would bind to cells that are "deeper" in the tumor, thus potentially giving rise to two distinct areas of cells, those penetrated by RTX and therefore subject to both RTX-mediated killing and the shaving reaction, and those areas of cells not yet exposed to RTX. This phenomenon is likely to occur after infusion of small amounts of RTX, which promotes an increase in the percentage of CD20-negative cells (Fig. 3*A*), presumably in layers of tumor closest to capillaries. In the present model and likely in most human cancers, the majority of cells in a tumor mass are primarily malignant cells, and therefore saturation of the potential killing/phagocytic capacity of endogenous macrophages or NK cells for mAb-opsonized cells would be anticipated, thus allowing for shaving. Additional clinical investigations are planned, based on obtaining either biopsies or fine-needle aspirates from patients with B cell lymphomas, before and after RTX therapy, to determine whether RTX infusion induces shaving of B cells in lymphoid tumors.

Several mouse models have demonstrated the ability of RTX, or other anti-CD20 mAbs, to effectively eliminate human B cell tumors or normal mouse B cells (10, 12–15, 18, 20, 22). The experiments we conducted in the present model were not designed to evaluate the cytotoxic action or therapeutic efficacy of RTX; we waited until tumors had already been established and were growing, and treatment with RTX was limited to brief periods, to determine whether shaving could indeed be demonstrated. Documentation of shaving in the present model replicates our previous findings in CLL (21, 25) and, taken together, these results indicate that under certain conditions cancer therapy with mAbs such as RTX may be only partially effective, due to limiting factors independent of the dose of RTX or its concentration in the bloodstream.

We suggest that if the cytotoxic actions of an anti-tumor mAb require and are limited to effector functions provided by the host, such as ADCC or CDC, then when these mechanisms are saturated, depleted, and/or unavailable, dosing with additional mAb may not be effective. In such cases, treatment with more mAb may be counterproductive, if shaving occurs instead. The shaving reaction is quite similar to antigenic modulation, first documented in cancer immunotherapy >25 years ago (56–58). Paradigms designed to address these issues may lead to new and improved therapeutic modalities. Such approaches may include repeated dosing with small amounts of RTX over extended time periods (21) as well as selectively down-modulating the shaving reaction, based on either treatment with IVIG or with small molecules that block endocytosis (59–61). Alternative strategies which could address the issue of saturation of effector cell-killing mechanisms would include serial transplantations of large numbers of autologous or donor-compatible NK cells (62–64) which could allow for substantially enhanced killing of RTX-opsonized neoplastic B cells in tumors.

Acknowledgment

We thank Dr. David Mack for critical reading of this manuscript.

Disclosures

Michael E. Williams has received research support for other projects from Biogen IDEC and Genentech and is a member of the continuing medical education speakers' bureaus sponsored by these corporations.

References

1. Maloney, D. G., A. J. Grillo-López, C. A. White, D. Bodkin, R. J. Schilder, J. A. Neidhart, N. Janakiraman, K. A. Foon, T. Liles, B. K. Dallaire, et al. 1997. IDEC-C2B8 (rituximab) anti-CD20 monoclonal antibody therapy in patients with relapsed low-grade non-Hodgkin's lymphoma. *Blood* 90: 2188–2195.
2. McLaughlin, P., A. J. Grillo-Lopez, B. K. Link, R. Levy, M. S. Czuczman, M. E. Williams, M. R. Heyman, I. Bence-Bruckler, C. A. White, F. Cabanillas, et al. 1998. Rituximab chimeric anti-CD20 monoclonal antibody therapy for relapsed indolent lymphoma: half of patients respond to a four-dose treatment program. *J. Clin. Oncol.* 16: 2825–2833.
3. Carter, P. 2001. Improving the efficacy of antibody-based cancer therapies. *Nature* 1: 118–129.
4. Glennie, M. J., and J. G. J. van de Winkel. 2003. Renaissance of cancer therapeutic antibodies. *Drug Discovery Today* 8: 503–509.
5. Stern, M., and R. Herrmann. 2005. Overview of monoclonal antibodies in cancer therapy: present and promise. *Crit. Rev. Oncol. Hematol.* 54: 11–29.
6. Cheson, B. D. 2006. Monoclonal antibody therapy of chronic lymphocytic leukemia. *Cancer Immunol. Immunother.* 55: 188–196.
7. Carter, P. J. 2006. Potent antibody therapeutics by design. *Nat. Rev. Immunol.* 6: 343–357.
8. Scallon, B. J., L. A. Snyder, G. M. Anderson, Q. Chen, L. Yan, L. M. Weiner, and M. T. Nakada. 2006. A review of antibody therapeutics and antibody-related technologies for oncology. *J. Immunother.* 29: 351–364.
9. Reff, M. E., K. Carner, K. S. Chambers, P. C. Chinn, J. E. Leonard, R. Raab, R. A. Newman, N. Hanna, and D. R. Anderson. 1994. Depletion of B cells in vivo by a chimeric mouse human monoclonal antibody to CD20. *Blood* 83: 435–445.
10. Clynes, R. A., T. L. Towers, L. G. Presta, and J. V. Ravetch. 2000. Inhibitory Fc receptors modulate in vivo cytotoxicity against tumor targets. *Nat. Med.* 6: 443–446.
11. Johnson, P., and M. Glennie. 2003. The mechanisms of action of rituximab in the elimination of tumor cells. *Semin. Oncol.* 30: 3–8.
12. Gaetno, N. D., E. Cittera, R. Nota, A. Vecchi, V. Grieco, E. Scanziani, M. Botto, M. Introna, and J. Golay. 2003. Complement activation determines the therapeutic activity of rituximab in vivo. *J. Immunol.* 171: 1581–1587.
13. Uchida, J., Y. Hamaguchi, J. A. Oliver, J. V. Ravetch, J. C. Poe, K. M. Haas, and T. F. Tedder. 2004. The innate mononuclear phagocyte network depletes B lymphocytes through Fc receptor-dependent mechanisms during anti-CD20 antibody immunotherapy. *J. Exp. Med.* 199: 1659–1669.
14. Cragg, M. S., and M. J. Glennie. 2004. Antibody specificity controls in vivo effector mechanisms of anti-CD20 reagents. *Blood* 103: 2738–2743.

15. Gong, Q., Q. Ou, S. Ye, W. P. Lee, J. Cornelius, L. Diehl, W. Y. Lin, Z. Hu, Y. Lu, Y. Chen, et al. 2005. Importance of cellular microenvironment and circulatory dynamics in B cell immunotherapy. *J. Immunol.* 174: 817–826.
16. Cragg, M. S., C. A. Walshe, A. O. Ivanov, and M. J. Glennie. 2005. The biology of CD20 and its potential as a target for monoclonal antibody therapy. *Curr. Dir. Autoimmun.* 8: 140–174.
17. Lefebvre, M.-L., S. W. Krause, M. Salcedo, and A. Nardin. 2006. Ex vivo-activated human macrophages kill chronic lymphocytic leukemia cells in the presence of rituximab: mechanism of antibody-dependent cellular cytotoxicity and impact of human serum. *J. Immunother.* 29: 388–397.
18. Golay, J., E. Cittera, N. Di Gaetano, M. Manganini, M. Mosca, M. Nebuloni, N. van Rooijen, L. Vago, and M. Introna. 2006. The role of complement in the therapeutic activity of rituximab in a murine B lymphoma model homing in lymph nodes. *Hematologica* 91: 176–183.
19. van Meerten, T., R. S. van Rijn, S. Hol, A. Hagenbeek, and S. B. Ebeling. 2006. Complement-induced cell death by rituximab depends on CD20 expression level and acts complementary to antibody-dependent cellular cytotoxicity. *Clin. Cancer Res.* 12: 4027–4035.
20. Hamaguchi, Y., Y. Xiu, K. Komura, F. Nimmerjahn, and T. F. Tedder. 2006. Antibody isotype-specific engagement of Fcγ receptors regulates B lymphocyte depletion during CD20 immunotherapy. *J. Exp. Med.* 203: 743–753.
21. Williams, M. E., J. J. Densmore, A. W. Pawluczkowycz, P. V. Beum, A. D. Kennedy, M. A. Lindorfer, S. H. Hamil, J. C. Eggleton, and R. P. Taylor. 2006. Thrice-weekly low-dose rituximab decreases CD20 loss via shaving and promotes enhanced targeting in chronic lymphocytic leukemia. *J. Immunol.* 177: 7435–7443.
22. Tedder, T. F., A. Baras, and Y. Xiu. 2006. Fcγ receptor-dependent effector mechanisms regulate CD19 and CD20 antibody immunotherapies for B lymphocyte malignancies and autoimmunity. *Springer Semin. Immunopathol.* 28: 351–364.
23. Huhn, D., C. von Schilling, M. Wilhelm, A. Ho, M. Hallek, R. Kuse, W. Knauf, U. Riedel, A. Hinke, S. Srock, et al. 2001. Rituximab therapy of patients with B cell chronic lymphocytic leukemia. *Blood* 98: 1326–1331.
24. Berinstein, N. L., A. J. Grillo-Lopez, C. A. White, I. Bence-Bruckler, D. Maloney, M. Czuczman, D. Green, J. Rosenberg, P. McLaughlin, and D. Shen. 1998. Association of serum rituximab (IDEC-C2B8) concentration and anti-tumor response in the treatment of recurrent low-grade or follicular non-Hodgkin's lymphoma. *Ann. Oncol.* 9: 995–1001.
25. Kennedy, A. D., P. V. Beum, M. D. Solga, D. J. DiLillo, M. A. Lindorfer, C. E. Hess, J. J. Densmore, M. E. Williams, and R. P. Taylor. 2004. Rituximab infusion promotes rapid complement depletion and acute CD20 loss in chronic lymphocytic leukemia. *J. Immunol.* 172: 3280–3288.
26. Beum, P. V., A. D. Kennedy, M. E. Williams, M. A. Lindorfer, and R. P. Taylor. 2006. The shaving reaction: rituximab/CD20 complexes are removed from mantle cell lymphoma and chronic lymphocytic leukemia cells by THP-1 monocytes. *J. Immunol.* 176: 2600–2609.
27. Estrov, Z., M. Talpaz, S. Ku, D. Harris, Q. Van, M. Beran, C. Hirsch-Ginsberg, Y. Huh, G. Yee, and R. Kurzrock. 1998. Z-138: a new mature B cell acute lymphoblastic leukemia cell line from a patient with transformed chronic lymphocytic leukemia. *Leuk. Res.* 22: 341–353.
28. Tucker, C. A., G. Bebb, R. J. Klasa, M. Chhanabhai, V. Lestou, D. E. Horsman, R. D. Gascoyne, A. Wiestner, D. Masin, M. Bally, and M. E. Williams. 2006. Four human T (11,14)(q13;q32)-containing cell lines having classic and variant features of mantle cell lymphoma. *Leuk. Res.* 30: 449–457.
29. Medeiros, L. J., Z. Estrov, and G. Z. Rassidakis. 2006. Z-138 cell line was derived from a patient with blastoid variant mantle cell lymphoma. *Leuk. Res.* 30: 497–501.
30. Whipple, E. C., A. H. Ditto, R. S. Shanahan, J. R. Gatesman, S. F. Little, R. P. Taylor, and M. A. Lindorfer. 2007. Low doses of antigen coupled to anti-CR2 mAbs induce rapid and enduring IgG immune responses in mice and in cynomolgus monkeys. *Mol. Immunol.* 44: 377–388.
31. Kennedy, A. D., M. D. Solga, T. A. Schuman, A. W. Chi, M. A. Lindorfer, W. M. Sutherland, P. L. Foley, and R. P. Taylor. 2003. An anti-C3b(i) monoclonal antibody enhances complement activation, C3b(i) deposition, and killing of $CD20^+$ cells by rituximab. *Blood* 101: 1071–1079.
32. Taylor, R. P., E. L. Wright, and F. Pocanic. 1989. Quantitative analyses of C3b capture and immune adherence of IgM antibody/dsDNA immune complexes. *J. Immunol.* 143: 3626–3631.
33. Unkeless, J. C. 1979. Characterization of a monoclonal antibody directed against mouse macrophage and lymphocyte Fc receptors. *J. Exp. Med.* 150: 580–596.
34. Kurlander, R. J., D. M. Ellison, and J. Hall. 1984. The blockade of Fc receptor-mediated clearance of immune complexes in vivo by a monoclonal antibody (2.4G2) directed against Fc receptors on murine leukocytes. *J. Immunol.* 133: 855–862.
35. Yan, J., V. Vetvicka, Y. Xia, M. Hanikyrova, T. N. Mayadas, and G. D. Ross. 2000. Critical role of Kupffer cell CR3 (CD11b/CD18) in the clearance of IgM-opsonized erythrocytes or soluble β-glucan. *Immunopharmacology* 46: 39–54.
36. Song, S., A. R. Crow, J. Freedman, and A. H. Lazarus. 2003. Monoclonal IgG can ameliorate immune thrombocytopenia in a murine model of ITP: an alternative to IVIG. *Blood* 101: 3708–3713.
37. Wakeham, J., J. Wang, J. Magram, K. Croitoru, R. Harkness, P. Dunn, A. Zganiacz, and Z. Xing. 1998. Lack of both types 1 and 2 cytokines, tissue inflammatory responses, and immune protection during pulmonary infection by *Mycobacterium bovis* bacille Calmette-Guérin in IL-12-deficient mice. *J. Immunol.* 160: 6101–6111.
38. Saxena, R. K., D. Weissman, J. Simpson, and D. M. Lew. 2002. Murine model of BCG lung infection: dynamics of lymphocyte subpopulations in lung interstitium and tracheal lymph nodes. *J. Biosci.* 27: 143–153.
39. Whipple, E. C., R. S. Shanahan, A. H. Ditto, R. P. Taylor, and M. A. Lindorfer. 2004. Analyses of the in vivo trafficking of stoichiometric doses of an anti-complement receptor 1/2 monoclonal antibody infused i.v. in mice. *J. Immunol.* 173: 2297–2306.
40. Ghetie, M. A., J. Richardson, T. Tucker, D. Jones, J. Uhr, and E. Vietta. 1990. Disseminated or localized growth of a human B cell tumor (Daudi) in SCID mice. *Int. J. Cancer* 45: 481–485.
41. Ghetie, M. A., L. J. Picker, J. A. Richardson, K. Tucker, J. W. Uhr, and E. S. Vitetta. 1994. Anti-CD19 inhibits the growth of human B cell tumor lines in vitro and of Daudi cells in SCID mice by inducing cell cycle arrest. *Blood* 83: 1329–1336.
42. Gelderman, K. A., S. Tomlinson, G. D. Ross, and A. Gorter. 2004. Complement function in monoclonal antibody-mediated cancer immunotherapy. *Trends Immunol.* 25: 158–164.
43. Li, B., D. J. Allendorf, R. Hansen, J. Marroquin, C. Ding, D. E. Cramer, and J. Yan. 2006. Yeast β-glucan amplifies phagocyte killing of iC3b-opsonized tumor cells via complement receptor 3-Syk-PI3K pathway. *J. Immunol.* 177: 1661–1669.
44. Siragam, V., D. Brinc, A. D. Crow, S. Song, J. Freedman, and A. H. Lazarus. 2005. Can antibodies with specificity for soluble antigens mimic the therapeutic effects of intravenous IgG in the treatment of autoimmune disease? *J. Clin. Invest.* 115: 155–160.
45. Nimmerjahn, F., P. Bruhns, K. Horiuchi, and J. V. Ravetch. 2005. FcγRIV: a novel FcR with distinct IgG subclass specificity. *Immunity* 23: 41–51.
46. Cartron, G., L. Dacheux, G. Salles, P. Solal-Celigny, P. Bardos, P. Colombat, and H. Watier. 2002. Therapeutic activity of humanized anti-CD20 monoclonal antibody and polymorphism in IgG Fc receptor FcγRIIIa gene. *Blood* 99: 754–758.
47. Weng, W. K., and R. Levy. 2003. Two immunoglobulin G fragment C receptor polymorphisms independently predict response to rituximab in patients with follicular lymphoma. *J. Clin. Oncol.* 21: 3940–3947.
48. Dall'Ozzo, S., S. Tartas, G. Paintaud, G. Cartron, P. Colombat, P. Bardos, H. Watier, and G. Thibault. 2004. Rituximab-dependent cytotoxicity by natural killer cells: influence of FCGR3A polymorphism on the concentration-effect relationship. *Cancer Res.* 64: 4664–4669.
49. Bowles, J. A., and G. J. Weiner. 2005. CD16 polymorphisms and NK activation induced by monoclonal antibody-coated target cells. *J. Immunol. Methods* 304: 88–99.
50. Fischer, L., O. Penack, C. Gentilini, A. Nogai, A. Muessig, E. Thiel, and L. Uharek. 2006. The anti-lymphoma effect of antibody-mediated immunotherapy is based on an increased degranulation of peripheral blood natural killer (NK) cells. *Exp. Hematol.* 34: 753–759.
51. Schreiber, A. D., and M. M. Frank. 1972. Role of antibody and complement in the immune clearance and destruction of erythrocytes: in vivo effects of IgG and IgM complement fixing sites. *J. Clin. Invest.* 51: 575–582.
52. Kimberly, R. P., T. M. Parris, R. D. Inman, and J. S. Mcdougal. 1983. Dynamics of mononuclear phagocyte system Fc receptor function in systemic lupus erythematosus: relation to disease activity and circulating immune complexes. *Clin. Exp. Immunol.* 51: 261–268.
53. Song, S., A. R. Crow, V. Siragam, J. Freedman, and A. H. Lazarus. 2005. Monoclonal antibodies that mimic the action of anti-D in the amelioration of murine ITP act by a mechanism distinct from that of IVIg. *Blood* 105: 1546–1548.
54. Fujimori, K., D. G. Covell, J. E. Fletcher, and J. N. Weinstein. 1989. Modeling analysis of the global and microscopic distribution of immunoglobulin G, $F(ab')_2$ and Fab in tumors. *Cancer Res.* 49: 5656–5663.
55. Adams, G. P., R. Schier, A. M. McCall, H. H. Simmons, E. M. Horak, R. K. Alpqugh, J. D. Marks, and L. M. Weiner. 2001. High affinity restricts the localization and tumor penetration of single-chain Fv antibody molecules. *Cancer Res.* 61: 4750–4755.
56. Ritz, J., J. M. Pesando, S. E. Sallan, L. A. Clavell, J. Notis-McConarty, P. Rosenthal, and S. F. Schlossman. 1981. Serotherapy of acute lymphoblastic leukemia with monoclonal antibody. *Blood* 58: 141–152.
57. Rinnooy Kan, E. A., E. Platzer, K. Welte, and C. Y. Wang. 1984. Modulation induction of the T3 antigen by OKT3 antibody is monocyte dependent. *J. Immunol.* 133: 2979–2985.
58. Schroff, R. W., M. M. Farrell, R. A. Klein, H. C. Stevenson, and N. L. Warner. 1985. Induction and enhancement by monocytes of antibody-induced modulation of a variety of human lymphoid cell surface antigens. *Blood* 66: 620–626.
59. Booth, J. W., M. K. Kim, A. Jankowski, A. D. Schreiber, and S. Grinstein. 2002. Contrasting requirements for ubiquitylation during Fc receptor-mediated endocytosis and phagocytosis. *EMBO J.* 21: 251–258.
60. Hoppe, H. C., D. A. van Schalkwyk, U. I. M. Wiehart, S. A. Meredith, J. Egan, and B. W. Weber. 2004. Antimalarial quinolines and artemisinin inhibit endocytosis in *Plasmodium falciparum*. *Antimicrob. Agents Chemother.* 48: 2370–2378.
61. Sarkar, K., M. J. Kruhlak, S. L. Erlandsen, and S. Shaw. 2005. Selective inhibition by rottlerin of macropinocytosis in monocyte-derived dendritic cells. *Immunology* 116: 513–524.
62. Klingemann, H. G. 2005. NK cell-based immunotherapeutic strategies. *Cytotherapy* 7: 16–22.
63. Leung, W., R. Iyengar, T. Leimig, M. S. Holladay, J. Houston, and R. Handgretinger. 2005. Phenotype and function of human natural killer cells purified by using a clinical-scale immunomagnetic method. *Cancer Immunol. Immunother.* 54: 389–394.
64. Clemenceau, B., G. Gallot, R. Vivien, J. Gaschet, M. Campone, and H. Vie. 2006. Long-term preservation of antibody-dependent cellular cytotoxicity (ADCC) of natural killer cells amplified in vitro from the peripheral blood of breast cancer patients after chemotherapy. *J. Immunother.* 29: 53–60.